In-solution enrichment identifies peptide inhibitors of protein–protein interactions

HHS Public Access

Author manuscript

Nat Chem Biol. Author manuscript; available in PMC 2019 August 26.

Published in final edited form as:

Nat Chem Biol. 2019 April ; 15(4): 410–418. doi:10.1038/s41589-019-0245-2.

In-solution enrichment identifies peptide inhibitors of protein–protein interactions

Fayçal Touti[1,*], **Zachary P. Gates**[1], **Anupam Bandyopdhyay**[1], **Guillaume Lautrette**[1], **Bradley L. Pentelute**[1,2,*]

[1]Department of Chemistry, Massachusetts Institute of Technology, Cambridge, MA, USA.

[2]Koch Institute, Broad Institute of Harvard and MIT, Center for Environmental Health Sciences, Massachusetts Institute of Technology, Cambridge, MA, USA.

Abstract

The use of competitive inhibitors to disrupt protein–protein interactions (PPIs) holds great promise for the treatment of disease. However, the discovery of high-affinity inhibitors can be a challenge. Here we report a platform for improving the affinity of peptide-based PPI inhibitors using non-canonical amino acids. The platform utilizes size exclusion-based enrichment from pools of synthetic peptides (1.5–4kDa) and liquid chromatography-tandem mass spectrometry-based peptide sequencing to identify high-affinity binders to protein targets, without the need for 'reporter' or 'encoding' tags. Using this approach—which is inherently selective for high-affinity binders—we realized gains in affinity of up to ~100- or ~30-fold for binders to the oncogenic ubiquitin ligase MDM2 or HIV capsid protein C-terminal domain, which inhibit MDM2-p53 interaction or HIV capsid protein C-terminal domain dimerization, respectively. Subsequent macrocyclization of select MDM2 inhibitors rendered them cell permeable and cytotoxic toward cancer cells, demonstrating the utility of the identified compounds as functional PPI inhibitors.

Disruption of PPIs is a major focus in drug discovery[1,2]. With more than 400,000 PPIs, the human interactome provides a wealth of opportunities for therapeutic intervention in a range of disease conditions. Peptides have played an important role in guiding the design of small-molecule inhibitors and in certain cases have served as the drug itself[3]. Research into these peptide-based drugs has gained momentum[4,5] for numerous reasons, including the

[*]**Correspondence and requests for materials** should be addressed to F.T. or B.L.P. faycaltouti@gmail.com; blp@mit.edu.

Author contributions

F.T. and B.L.P. conceived the study with input from Z.P.G. F.T. and B.L.P. directed the project and designed experiments. F.T. performed most experiments. Z.P.G. and A.B. contributed to OBOC screen design and experiments, and G.L. contributed to library purification and binder validation. F.T., Z.P.G., and B.L.P. wrote the manuscript. All authors contributed to the analysis, interpretation, and validation of the data.

Competing interests

A patent application covering this work has been filed by MIT-TLO.

Supplementary information is available for this paper at https://doi.org/10.1038/s41589-019-0245-2.

Online content

Any methods, additional references, Nature Research reporting summaries, source data, statements of data availability and associated accession codes are available at https://doi.org/10.1038/s41589-019-0245-2.

development of new synthetic methods for the preparation of peptide macrocycles and peptidomimetics with improved pharmacological properties[6-8].

Disrupting PPIs remains a challenge owing to their large and featureless surfaces. The discovery of 'hotspot' regions that contribute substantially to the free energy of binding has facilitated the rational design of PPI inhibitors. However, molecular dissection of PPIs has revealed that contacts are often suboptimal[3,9,10]. Non-canonical amino acids have the potential to optimize binding contacts, and to yield inhibitors with improved metabolic stability and superior physicochemical properties[4,5]. A combination of in silico and empirical methods have been used to identify peptide binders that contain non-canonical amino acids[9-13].

Recently, combinatorial approaches have been applied to discover novel peptide variants that inhibit PPIs[14,15]. Affinity selection from synthetic peptide pools is a promising technique for controlling the affinity of identified peptide ligands[16,17], and is widely used in the pharmaceutical industry for discovery of small-molecule ligands with low false-positive rates[18-20]. However, its application to peptides has been limited to the screening of pools containing fewer than 20 compounds, due in part to the challenge of sequencing the complex peptide mixtures that would result from screening larger pools[17,21]. Recent advances in commercial mass spectrometers and high-throughput peptide sequencing therefore open up the possibility of revisiting affinity selection to screen synthetic libraries[22].

With the goal of discovering improved peptide-based PPI inhibitors using non-canonical amino acids, we developed a solution-based affinity selection platform to identify binders from pools of 10^3–10^6 synthetic peptides. The oncogenic ubiquitin ligase MDM2 was used as a benchmark protein target. Starting from a known MDM2 binder that inhibits the MDM2–p53 interaction, we prepared focused libraries in which hotspot residues were randomized, and used these libraries to explore the utility of non-canonical amino acids for improving binding affinity. This approach allowed for the identification of a number of high-affinity, unnatural ligands that were further engineered into macrocyclic disruptors of the p53–MDM2 interaction. An analogous approach was used to identify improved binders to C-CA. Taken together, the results illustrate the utility of affinity selection for the screening of synthetic peptide libraries, and the value of non-canonical amino acids for engineering high-affinity peptide-based PPI inhibitors.

Results

Affinity selection enables enrichment and sequencing of peptide binders.

Drawing from seminal work in the field of affinity selection coupled to mass spectrometry, in which small-molecule library members are usually encoded with unique masses[17,18,21,23,24], we developed a platform based on liquid chromatography–tandem mass spectrometry sequencing (LC–MS/MS) of peptides coupled with high-performance and high-pressure size exclusion chromatography (HPSEC, Fig. 1). The HPSEC assay was investigated with different inhibitors including linear peptides, macrocyclic peptides, and miniproteins. Our goal was to establish methods for HPSEC to differentiate protein-bound

versus unbound peptides and determine the conditions required for de novo sequencing by LC–MS/MS.

For peptide-based binders to trypsin, anti-Flag mAb, MDM2, and C-CA (Supplementary Table 1), protein-dependent detection in the 'breakthrough fraction' was observed, demonstrating the potential of this HPSEC setup for selecting functional ligands (Supplementary Fig. 1). Nanomolar affinity binders were preferentially retained in the breakthrough fraction with yields of 15–24% (Supplementary Table 2 and Supplementary Fig. 2). Postselection tandem mass spectrometry (MS/MS) sequencing of linear binders was illustrated with the MDM2 system. In this case, for both an individual nanomolar affinity binder and a focused library of 10^3 members, 6 nM peptide concentration was sufficient for sequencing, suggesting that this assay could potentially select binders from pools as large as 10^6 members, before reaching a solubility limit of the total peptide concentration (Supplementary Figs. 3-6).

To enable MS/MS-based sequencing of non-natural scaffolds, including peptide macrocycles and cystine knot miniproteins, we developed chemical strategies to linearize the binding sequences (Supplementary Fig. 7). These strategies are illustrated by a perfluoroarylsulfone-macrocyclized binder of MDM2, for which treatment with nucleophiles enabled postselection excision of the sulfone containing linker, and with the cystine knot EETI-II, for which the use of a non-canonical diol amino acid enabled oxidative backbone cleavage of the trypsin-binding loop (Supplementary Figs. 8-10). These examples suggest that affinity selection is compatible with postselection transformations, and can be extended to nonlinear unnatural scaffolds that would be otherwise incompatible with MS/MS-based sequencing.

Affinity selection identifies hotspots of MDM2-binding peptides.

P53-like peptides that bind the MDM2 oncoprotein[25,26] with micromolar to nanomolar affinities were reported in the 1990s (ref. [25]), and the basis of their molecular interaction with MDM2 has been dissected using Ala-scanning[27] and phage display[28]. To benchmark our affinity selection approach, library 1 (LTXXHXXAXXTSK, where X is a randomized residue; Fig. 2a and Supplementary Fig. 11) was prepared based on peptide dual inhibitor (pDI) (**1**, LTFEHYWAQLTSK), a peptide that binds MDM2 with nanomolar affinity[29] (47 nM or 25 nM using bio-layer interferometry (BLI) or a competition binding assay, respectively; Fig. 2). This 10^6-member library was subjected to in-solution enrichment (Fig. 2b and Supplementary Figs. 12 and 13), which identified 18 putative binders in a single experiment (Supplementary Fig. 13). These sequences were found to have in common the FWL triad (Fig. 2b and Supplementary Fig. 13), confirming earlier results[28,30] showing that these residues are the hotspots required for binding to MDM2. Four randomly selected putative binders were synthesized in biotinylated form, and evaluated for MDM2 binding in a BLI assay (Fig. 2b). Affinities of 45–120 nM were obtained, confirming the propensity of affinity selection to identify binders in this range of affinities (Fig. 2b).

The mutational tolerance of pDI hotspots was further investigated with focused library 2 (LTXEHYXAQXTSK, where X is a randomized residue; Fig. 2a) to provide molecular insights into pDI binding to MDM2. Affinity selection experiments were conducted with increased library 2 amounts and allowed for the recovery of binders with a wider range of

affinities (Supplementary Figs. 14 and 15). Five sequences (Supplementary Fig. 16) were identified including reference compound pDI (**1**). These were resynthesized for validation (6–10, Fig. 2c). For all variants, tryptophan was conserved at position 7, suggesting that this residue imparts the highest binding energy contribution, a well-known result for p53-derived binders[27,30]. The mutation of Leu to Phe (**6**) at position 10 produced a nanomolar binder, showing that the MDM2 pocket can accommodate larger hydrophobic residues at this position. By contrast, for both positions 3 and 10, mutation to Tyr (**8** and **9**) or to Leu (**10**) appreciably weakened MDM2 binding (Fig. 2c). Taken together, these results demonstrate the capability of the affinity selection approach to confirm the determinants of pDI-MDM2 interaction and suggest that, using canonical amino acids alone, mutations to pDI hotspots have either neutral or deleterious effects.

MDM2 hotspots tolerate a variety of unnatural residues.

To determine the compatibility of the MDM2 interface with non-canonical amino acids, we prepared a focused pDI library (library 3, LTXEHYXAQXTSK, where X is a randomized residue; Fig. 3a) in which hotspots were randomized using commercially available non-canonical L-amino acids. Affinity selection led to the detection of hundreds of peptides from library 3, in contrast to only 2 for library 2 in comparable screening conditions (Supplementary Fig. 14), suggesting that non-canonical amino acids facilitate binding to the MDM2 pocket (Supplementary Table 3). Twenty-seven sequences were identified and sequenced by MS/MS with average local confidence scores >80% including reference pDI (Supplementary Table 3). Ten randomly chosen putative binders were selected, synthesized in acetylated form, and evaluated for MDM2 binding in a BLI assay (**11**–**20**, Supplementary Table 3). Affinities of 5–130 nM were observed, confirming again the preferential selection of nanomolar affinity binders using HPSEC under these conditions (Supplementary Table 3). For these sequences, pDI hotspots were partially or completely replaced by non-canonical amino acids, thereby illustrating the potential of the affinity selection method for discovery of peptide variants with unnatural residues (Supplementary Table 3).

Affinity selection samples a narrow range of affinities compared with one-bead one-compound (OBOC).

The OBOC approach is an established technology capable of screening synthetic libraries containing non-canonical amino acids[31,32]. To evaluate the performance of our affinity selection approach relative to this method, we prepared bead-based OBOC library 3, sharing the same design features as library 3 (Fig. 3a). OBOC library 3 was prepared on beads uniformly attenuated to 5% amine loading[33], and screened against biotinylated MDM2 using streptavidin alkaline phosphatase (SA-AP) detection[34,35]. Two procedures were employed: a ‘direct staining’ approach, in which library beads were incubated with tetrameric MDM2-SA-AP, and an ‘indirect staining’ approach, in which library beads were incubated with biotinylated MDM2, washed stringently, and then incubated with SA-AP[36]. In both cases, ~50 positive beads were selected for sequencing; tens of putative binders were identified using LC–MS/MS, including the positive control pDI (Supplementary Figs. 17 and 18).

Side-by-side analysis of the putative binders identified by affinity selection versus bead-based screening revealed marked differences in non-canonical amino acid frequencies,

especially at position 7 (hotspot 2; Supplementary Fig. 19b). For the 'direct' bead-based screen, ten sequences were selected randomly for synthesis and binding assay (**21**–**30**, Supplementary Fig. 17). For the 'indirect' bead-based screen (Supplementary Fig. 18), 13 of 25 total sequences had either been identified elsewhere—and were of characterized affinity—or were closely related to a characterized sequence (Supplementary Fig. 18 and Supplementary Tables 3 and 4); 7 additional sequences were chosen for synthesis and binding validation (**31**–**36**, Supplementary Fig. 18), such that binding affinities would be obtained for ~75% of sequences from the indirect bead-based screen.

Putative binders identified by the bead-based screens exhibited a broad range of affinities from 0.5 nM to >5 μM. Indirect staining identified a greater proportion of high-affinity binders compared with direct staining (Supplementary Fig. 19c), including the 2 highest-affinity MDM2 binders identified in this work (**37** and **39**, Supplementary Table 4); however, for each bead-based screen, ~30% of identified binders were of micromolar affinity or weaker (Supplementary Figs. 17, 18, and 19c). In contrast, affinity selection identified high-affinity sequences only (K_d < 150 nM) (Supplementary Fig. 19c and Supplementary Table 3), consistent with the narrow dispersion of monomers at position 7 (Supplementary Fig. 19b). These results demonstrate the ability of HPSEC to sample a narrower range of affinities, and to accurately identify residues associated with high-affinity binding.

To confirm the propensity of the on-bead assay to identify MDM2 ligands spanning a wide range of binding affinities, select positive controls (K_d = 2.5 μM, 47 nM, or 0.5 nM) were synthesized on-bead for evaluation in on-bead binding assays using the direct staining approach (Supplementary Fig. 20). These samples gave comparable positive outcomes across a range of MDM2 concentrations (Supplementary Fig. 20), consistent with both the wide distribution of binding affinities identified by the OBOC screen conducted here (Supplementary Fig. 19c), as well as the micromolar affinity of MDM2 ligands reported for other bead-based screens[14,37,38]. Many parameters—including protein target concentration, bead loading, and the presence of soluble competing ligands—may influence the outcome of on-bead binding assay[35], and, potentially, conditions that completely abrogate the identification of weaker-affinity ligands could be found. However, our data support the conclusion that under typical conditions, and in the absence of soluble competitors, affinity selection samples ligands over a narrower range of higher affinities. This result suggests complementary roles for affinity selection and bead-based screening in combinatorial discovery: beads are best suited for de novo discovery from diverse libraries, where isolation of weak binders is a challenge, whereas affinity selection is best suited for generation of focused libraries to improve affinity once a lead compound has been discovered.

Competitive affinity selection identifies high-affinity binders to MDM2.

With the goal to discover abiotic binders to MDM2 with affinities superior to pDI, we examined library 3 under competitive affinity selection conditions. First, we examined the effect of an exogenous binding competitor on the selection outcome (Fig. 3b and Supplementary Fig. 21). Addition of 100 μM of pDI to this library decreased the number of detected sequences from 261 to 96 (Fig. 3b and Supplementary Fig. 21). Twenty non-canonical sequences identified under competitive conditions were synthesized and validated

for binding using BLI (**37**–**58**, Fig. 3c and Supplementary Table 4). A number of sequences exhibited equivalent or improved binding affinity compared with pDI, demonstrating the utility of competitive conditions for controlling the affinity of identified binders (Supplementary Fig. 21 and Supplementary Table 4).

These experiments indicated that Trp7 can be replaced by the flexible and hydrophobic hexylalanine (**37**, **41**–**47**, **52**, and **53**), the bulky anthrylalanine (**51**), or the 2-naphthylalanine residues (**56** and **57**) to yield nanomolar binders to MDM2. These findings underline the features of the MDM2 binding pocket around this hotspot and suggest that these residues have different binding modes than Trp, for which indole nitrogen is involved in a hydrogen bond with MDM2 backbone[27,39] (Fig. 3c and Supplementary Table 4). Additionally, replacement of Trp with an inert side chain such as hexylalanine may be useful for metabolic stability since Trp is prone to degradation[40]. Phe at position 3 was replaced by the more hydrophobic fluorinated phenylalanines, while Leu at position 10 was replaced by bulkier hydrophobic side chains including cyclobutylalanine (**37**, **39**, **42**, **51**, and **56**), cyclohexylalanine (**41**, **45**, and **49**), or fluorinated phenylalanines (**43**, **44**, **47**, **52**–**55**, and **57**; Supplementary Table 4).

We further decreased MDM2 concentration to increase the selection stringency. When MDM2 concentration was reduced 5-fold in the presence of 100 μM pDI, only 1 sequence was identified (corresponding to compound **37**). This sequence was the tightest MDM2 binder identified, with a K_d of 0.5 nM or 0.8 nM, as determined by BLI or a competition binding assay, respectively (Fig. 3c,d). Several subnanomolar affinity binders to MDM2 are known, including D-configured ^{D}PMI-β (ref. [12]) L-configured macrocyclic ATSP-7041 (ref. [41]), and a variant of the linear L-peptide PMI[27]. Interestingly, **37** also retained its binding for MDMX—a promising finding for the potential design of dual inhibitors (Supplementary Table 4). This is in contrast to ^{D}PMI-β, which exhibits lower affinity for MDMX[12].

Unnatural residues improve the affinity of a C-CA binder.

C-CA is an important target in the context of drug discovery[42]. Phage display-discovered peptide CAI (**59**), a micromolar allosteric binder to C-CA that inhibits the dimeric interface of the HIV capsid protein[43], has not found application in the clinic in part due to its low affinity[42]. Efforts to improve the affinity of **59** via synthetic libraries have not been reported. Therefore, we set out to improve the affinity of **59** by the use of non-canonical amino acids.

As in the case of pDI, a synthetic library based on CAI was prepared with hotspots[44] randomized with non-canonical amino acids (library 4, ITXEDXLHXXGPK, where X represents randomized residues; ~28,000 members; Supplementary Fig. 22a). Affinity selections with C-CA identified both new sequences and **59**, the phage-reported peptide (Supplementary Fig. 22b). Seven library members were synthesized and evaluated. Replacement of Phe3 by difluorophenylalanine (Supplementary Fig. 22b) and Leu5 by cyclobutylalanine yielded **60**, a nanomolar binder to C-CA with a 25-fold increase in affinity (Supplementary Fig. 22c). These results suggest that affinity selection can be extended to protein targets other than MDM2 and with starting ligands of micromolar affinity.

We attempted to perform an OBOC bead-based screen for C-CA, as described above for MDM2, to side-by-side compare the two methods. However, the preparation of a functional staining reagent based on C-CA was not feasible. In this case, binding of biotinylated C-CA to its ligand CAI was abrogated on complexation with SA-AP, complicating bead screens using this protein target (Supplementary Fig. 23). These data underline an additional advantage of affinity selection: the ability to screen a protein target without the need for 'reporter' labels or tags, which could perturb the structure or function of the protein.

Affinity selection identifies cystine knot fusions that bind MDM2.

With the aim to extend the affinity selection approach to other unnatural scaffolds, we tested the capability of HPSEC to select high-molecular-weight peptide binders (~4 kDa) from synthetic pools with protein targets (~23 kDa). As proof of concept, we designed an unnatural cystine knot fusion peptide (Fig. 4a) composed of a D-polypeptide binder of MDM2[12] fused to the N terminus of a D-configured cystine-stabilized beta sheet[45] variant of EETI-II (Fig. 4a). This variant was prepared by solid-phase peptide synthesis (SPPS) and oxidized to **78**, which contains 2 disulfide bonds (Supplementary Fig. 24). Using a label-free BLI assay, the affinity of **78** for MDM2 was estimated to be 20-fold weaker than **79**, the parent ^{D}PMI-β-based linear binder (Supplementary Table 5). Therefore, we set out to improve its affinity by selection from a synthetic cysteine knot fusion library.

Toward this goal, we designed D-library 5 (kaxyanxeklxr(Diol)ggsβ-$^{9–28}$EETI-II; Fig. 4b), where lowercase letters represent D-amino acids, x represents randomized residues, 'β' is a beta alanine residue, and 'Diol' is a non-canonical amino acid[46] that enables cleavage of the randomized N-terminal peptide from the fusion construct for MS/MS sequencing (Fig. 4c and Supplementary Fig. 25). Library 5 was synthesized, folded in solution, and subjected to affinity selection using SUMO-$^{25–109}$MDM2. We enriched for 18 putative binders after diol cleavage (Supplementary Fig. 26 and Supplementary Tables 5 and 6). For each putative binder, the *m/z* values before diol cleavage were consistent with the presence of disulfide bonds, confirming the correct folding of the knottin structure (Supplementary Table 6).

Ten sequences and controls were synthesized, folded, and investigated for binding, and found to have nanomolar affinities for MDM2 (**68**–**80**, Supplementary Table 5). Peptide **68** exhibited a 20-fold increase in binding affinity compared with **78**, and, similar to many other investigated binders, its central hotspot was an alkylalanine (Fig. 4d and Supplementary Table 5), further supporting the hypothesis that this flexible and hydrophobic side chain is equally efficient at binding the MDM2 pocket with high affinities in both L- and D-configurations. In contrast, Trp3 was conserved while Leu10 was replaced by bulkier hydrophobic side chains, paralleling results for the L-configured library 3. These data demonstrate that the affinity selection approach is capable of identifying high-molecular-weight unnatural miniprotein binders that inhibit PPIs with high affinity.

Cyclization of linear inhibitors affords PPI disruptors.

The discovery of functional compounds to inhibit PPIs has benefited from the development of macrocyclization chemistries[6-8] that can render peptides stable toward proteolysis and cell penetrating. To turn unnatural linear sequences into functional PPIs, we macrocyclized

several high-affinity inhibitors identified from libraries 3 and 4 using established chemical transformations such as ring-closing metathesis (RCM) and nitrogen arylation (Fig. 5a,b).

Using the *i*, *i* + 4 macrocyclization scheme[6-8,47], C-CA binding sequences were macrocyclized (**81**–**85**, Supplementary Fig. 27) and **82**, a macrocyclic C-CA binder with tighter binding than the reference bioactive NYAD (**85**), was identified (Supplementary Figure 27). In the case of MDM2, a subset of macrocyclized sequences from library 3 were found to have low-nanomolar affinities (**86**–**104**, Fig. 5b and Supplementary Table 7). These high-affinity inhibitors had in common the presence of difluorophenylalanine and cyclobutylalanine side chains while the central hotspot was a hexylalanine, naphthylalanine, or tryptophane residue (**86**, **87**, **90**, **91**, and **101**; Fig. 5b and Supplementary Table 7). Only peptides **90** and **91** retained affinity for MDM2 on perfluoroarylsulfone stapling (Fig. 5b and Supplementary Table 7).

We further evaluated the discovered macrocyclic low-nanomolar MDM2 binders **87** and **91** for their ability to cross cell membranes and reduce the viability of MDM2-overexpressing cell lines (Fig. 5c). In contrast to linear controls **107** and **108** (Fig. 5c), fluoresceinconjugated macrocyclic peptides (**105**, **106**, **110**, **111**, and **112**) and linear **109** showed appreciable intracellular signal as evidenced by confocal imaging and flow cytometry (Fig. 5d and Supplementary Figs. 28-31). However, only low-nanomolar-binding cell-permeant inhibitors were found to disrupt p53–MDM2 at levels comparable to positive controls ATSP-7041 and Nutlin-3 (refs.[26,41,48]), as evidenced by western blot analysis of p21 and MDM2 markers (Supplementary Figs. 32-36); this feature translated into a potent killing of SJSA-1 cells (Fig. 5e and Supplementary Fig. 37). In contrast, macrocyclic compounds with lower affinities for MDM2 (including scrambled variants) or limited cell penetration did not appreciably diminish the viability of these cancer cells at low micromolar concentration (Fig. 5e, Supplementary Fig. 38, and Supplementary Table 7). Similarly, the treatment of MCF-7, a cell line expressing both MDM2 and MDMX, with these macrocyclic inhibitors also led to diminished viability (Supplementary Fig. 39). In contrast, no dose-dependent killing at low micromolar concentrations was observed for K-562, a cell line lacking p53 (Supplementary Figs. 35, 36, and 39). Taken together, these results suggest that **87** and **91** selectively kill MDM2-overexpressing cells by disruption of the p53–MDM2 interaction when cells are treated with low micromolar concentrations of these compounds.

Discussion

The utility of an affinity selection platform to identify binders from synthetic peptide pools has been demonstrated. The platform leverages both the ability of HPSEC to resolve peptides (up to 4 kDa) from protein targets as light as 23 kDa, and the capability of modern mass spectrometers to detect and sequence enriched analytes at subpicomolar level. Key attributes of the platform are the preferential selection for nanomolar affinity binders, and the ability to screen peptide libraries against protein targets without the need for peptide encoding tags or protein ‘reporter’ labels. As illustrated by the preparation and screening of focused libraries based on known ligands of MDM2 and C-CA, identification of high-affinity PPI disruptors containing non-canonical amino acids is one application of this

technology. Based on the gains in affinity realized here, we believe that non-canonical amino acids may be broadly useful for improving the affinity of peptide-based inhibitors.

A combination of library solubility, HPSEC yield, and LC–MS/MS sensitivity restricts the number of compounds that can be simultaneously screened by affinity selection to approximately 10^6. Due to this limitation, this technique is most suited to improving the affinity of known binders, rather than unbiased de novo discovery. Therefore, the approach is complimentary to biological display technologies, which are limited with respect to unnatural amino acids but can access libraries of greater diversity. With regard to improvement of known binders, affinity selection constitutes a straightforward alternative to other powerful synthetic library approaches such as OBOC and DNA chemically encoded libraries[49], which can potentially examine more diverse libraries at the cost of more elaborate synthetic procedures.

Interfacing the products of affinity selection with macrocyclization chemistries enabled the discovery of cell-penetrating, bioactive inhibitors and illustrates the utility of macrocyclic scaffolds for the disruption of PPIs. The affinity maturation approach should be equally applicable to macrocyclic inhibitors, given suitable lead compounds. This would require postenrichment linearization of the macrocycles for MS/MS-based sequencing, as illustrated with the diol amino acid and perfluoroarylsulfone linker studied here. In principle, postenrichment chemical transformations could expand the variety of molecular scaffolds amenable to screening and sequencing by affinity selection-mass spectrometry. With continued development, we anticipate that interfacing affinity selection with new synthetic methods may ultimately facilitate the discovery of binders based on high-molecular-weight scaffolds for inhibiting so-called undruggable PPIs.

Methods

Materials.

High-performance size exclusion chromatography columns BIO-SEC-3, 7.8 × 150 mm^2, 3 μm, 100 Å and BIO-SEC-3, 7.8 × 50 mm^2, 3 μm, 100 Å and analytical reverse phase–high pressure liquid chromoatography (RP-HPLC) columns Zorbax 300 SB-C3, 2.1 × 150 mm^2, 5 μm and Poroshell 300 SB-C3, 1.0 × 75 mm^2 were purchased from Agilent Technologies. H-Rink Amide-ChemMatrix resin was obtained from PCAS BioMatrix. Tentagel M NH_2 resin was obtained from Rapp Polymere. 1-[Bis(dimethylamino)methylene]-1H-1,2,3-triazolo[4,5-b]pyridinium-3-oxid-hexafluorophosphate (HATU), Fmoc-L-Arg(Pbf)-OH, Fmoc-L-His(Trt)-OH, Fmoc-L-Lys(Boc)-OH, Fmoc-L-Asp(tBu)-OH, Fmoc-L-Glu(tBu)-OH, Fmoc-L-Ser(tBu)-OH, Fmoc-D-Ser(tBu)-OH, Fmoc-L-Thr(tBu)-OH, Fmoc-L-Asn(Trt)-OH, Fmoc-L-Gln(Trt)-OH, Fmoc-L-Cys(Trt)-OH, Fmoc-L-Gly-OH, Fmoc-L-Ala-OH, Fmoc-D-Ala-OH, Fmoc-L-Val-OH, Fmoc-L-Leu-OH, Fmoc-D-Leu-OH, Fmoc-L-Met-OH, Fmoc-L-Phe-OH, Fmoc-D-Phe-OH, Fmoc-L-Tyr(tBu)-OH, Fmoc-D-Tyr(tBu)-OH, Fmoc-L-Trp(Boc)-OH, Fmoc-D-Trp(Boc)-OH, Fmoc-3-Ala(9-anthryl)-OH, Fmoc-L-Ala(2-naphthyl)-OH, Fmoc-D-Ala(2-naphthyl)-OH Fmoc-L-Ala(pyrenyl)-OH, Fmoc-Ala(β-cyclobutyl)-OH, Fmoc-β-cyclobutyl-D-Ala-OH, Fmoc-L-Cha-OH, Fmoc-D-Cha-OH Fmoc-L-Phe(4-F)-OH, Fmoc-L-HomoPhe-OH, Fmoc-L-Phe(3,4-Dimethoxy)-OH, Fmoc-L-Phg-OH, Fmoc-L-Phe(4-CN)-OH, Fmoc-L-Phe(4-NO2)-OH, Fmoc-L-Phe(4-NHBoc)-OH,

Fmoc-L-Phe(4-CF3)-OH, Fmoc-D-Phe(4-CF3)-OH Fmoc-L-Ala(4,4'-biphenyl)-OH, Fmoc-3,4-difluoro-L-Phe-OH, Fmoc-3,4-difluoro-D-Phe-OH, Fmoc-L-Phe(3,4,5-trifluoro)-OH, Fmoc-L-Phe(F)5-OH, Fmoc-D-Phe(F)5-OH, Fmoc-D-HomoLeu-OH, Fmoc-β-Ala-OH, Fmoc-L-Dap(Boc)-OH, and FITC isomer I were purchased from Chem-Impex International. Fmoc-Anon(2)-OH, Fmoc-D-Anon(2)-OH, and Fmoc-D-Adec(2)-OH were purchased from Watanabe Chemical Industries. Fmoc-(R)-2-(7-octenyl)Ala-OH, Fmoc-(S)-2-(4-pentenyl)Ala-OH, and Hoveyda–Grubbs Catalyst Second Generation were obtained from Sigma-Aldrich. Biotin-PEG_4-NHS was purchased from ChemPep. Peptide synthesis-grade N,N-dimethylformamide (DMF), dichloromethane (DCM), diethyl ether, and HPLC-grade acetonitrile were obtained from VWR International. All reactions were set up on the bench top open to air. Trypsin from bovine pancreas and monoclonal ANTI-FLAG M2 antibody were purchased from Sigma-Aldrich. Human $^{1–137}$MDMX and Human $^{1–118}$MDM2 were ordered from Abcam. SUMO-$^{25–109}$MDM2 and SUMO-C-CA proteins were expressed as previously described[50,51]. Diol amino acid and perfluoroarylsulfone electrophile were prepared as previously described[8,52]. All other materials and reagents were purchased from commercial sources and used as received. Water was deionized and used as is. Dimethylsulfoxide (DMSO)-d6 was purchased in sealed ampules from Cambridge Isotopes. ^{1}H and ^{13}C NMR spectra were recorded on a Brucker 400 MHz spectrometer and calibration was performed using residual DMSO-d5 (2.54 ppm) as an internal reference.

HPSEC general procedure.

High-performance size exclusion chromatograms were acquired using Agilent 1260 HPLC-UV instrument. Selections were performed using high-performance size exclusion column BIO-SEC-3, 7.8 × 150 mm^2, 3-μm particle size, and 100-Å pore size, except for library 4 in which case BIO-SEC-3, 7.8 × 50 mm^2, 3-μm particle size, and 100-Å pore size was used. Typically, after 1 h at room temperature, binding mixtures of 100 μl containing peptides or peptide libraries and protein targets were isocratically eluted in buffered mobile phase (25 mM Tris, 50 mM NaCl, pH 7.0–7.5, with or without L-arginine supplementation) at 1 ml min^{-1} flow rate for 15 min. Generally, the mobile phase was also used as the binding buffer, and systematically before each experiment a blank injection was performed consisting of a protein-only injection. During affinity selection experiments the breakthrough fraction (protein fraction) was monitored by UV (214 nm) and collected. The latter contained the protein–binder complexes, which were dissociated using 0.2% formic acid before characterization by LC–MS or LC–MS/MS using typically 3.3–20% of the total volume (typically 0.6 ml). Control conditions with either peptides or protein targets omitted were subjected to similar conditions. After each experiment size-exclusion chromatography (SEC) columns were cleaned with 1 or a combination of the following buffers: 0.5 M Na_2SO_4, pH 3.0; 50 mM phosphate, pH 7.0, 20% acetonitrile; 6 M urea, 25 mM Tris, pH 7.5. Mixtures with higher organic solvent content were also used to clean SEC columns.

LC–MS and LC–MS/MS analysis of breakthrough fractions.

Samples were analyzed by LC–MS 6550 ESI-Q-TOF using an Agilent Zorbax 300 SB-C3 (2.1 × 150 mm^2, 5-μm particle size). Mobile phases were 0.1% formic acid in water (solvent A) and 0.1% formic acid in acetonitrile (solvent B). Typically, linear gradients of 1 to 65% solvent B over 10 or 34 min (flow rate: 0.5 ml min^{-1}) were used to acquire LC–MS

chromatograms. LC–MS/MS analysis was performed using a linear gradient of 1 to 65% solvent B over 34 min (flow rate: 0.5 ml min^{-1}). Absolute MS/MS threshold was typically set to 10^4 counts and selected precursor ions were +3 charged. MS/MS spectra were imported and analyzed using PEAKS Studio software from Bioinformatics Solutions. Fixed post-translational modifications commonly used were amidation (C terminus, any residue, −0.98 Da), EETI-II ^{1}Gly-^{2}Cys (amidomethyl, N terminus, any residue, 217.0521 Da), and ^{1}Lys-^{2}Ala (N terminus, any residue, 199.1320 Da). Variable post-translational modifications commonly used were F_5f (Phe, 89.9528 Da), F_3f (Phe, 53.9717 Da), F_2f (Phe, 35.9811 Da), Ff (Phe, 17.9887 Da), CF_3f (Phe, 67.9873 Da), NH_2f (Phe, 15.0108 Da), NO_2f (Phe, 44.985 Da), CNf (Phe, 24.9952 Da), Phg (Phe, −14.0156 Da), Dmf (Phe, 60.0211 Da), Homof (Phe, 14.0156 Da), Phf (Phe, 76.313 Da), Cha (Leu, 40.0313 Da), Hexa (Leu, 42.047 Da), Hepa (Leu, 56.047 Da), Homol (Leu, 14.0157 Da) Cba (Leu, 12.0 Da), Anta (Phe, 100.0313 Da), Pyra (Phe, 124.0313 Da), Napha (Phe, 50.0156 Da), methionine sulfoxide (Met, 15.9949 Da), and cleaved diol (C terminus, any residue, 70.0531 Da).

Peptide and peptide library preparation.

Manual solid-phase synthesis of non-canonical amino acid-containing peptides.—

Peptide sequences were manually synthesized typically at 0.05-mmol scale on H-Rink Amide-ChemMatrix resin using manual Fmoc-SPPS. Torviq syringes (10 ml) were utilized as the reactor vessel and the resin was swollen in DMF for a few minutes before starting peptide assembly. The procedure for canonical amino acid coupling cycle included 10-min coupling with Fmoc-protected amino acid (1 mmol, 20 equivalents), HATU (0.95 mmol, 19 equivalents, 0.38 M solution), and diisopropylethyl amine (DIEA; 500 µl, 100 equivalents) in DMF (2.5 ml) at room temperature. For non-canonical amino acids, 30-min couplings were performed with Fmoc-protected amino acids (0.25 mmol, 5 equivalents), HATU (0.237 mmol, 4.75 equivalents, 0.38 M solution), and DIEA (125 µl, 25 equivalents) in DMF (625 µl) at room temperature. The resin was periodically stirred during coupling then washed (5×) with DMF, deprotected (2×) for 3 min with 20% (*v/v*) piperidine in DMF, and finally washed again (5×) with DMF to conclude the cycle. After peptide synthesis completion, the resin was washed with DCM (5×) and dried under reduced pressure.

Automated fast-flow peptide synthesis.—

L- and D-configured peptide sequences containing usual amino acid side chains were synthesized at 90 °C on H-Rink Amide-ChemMatrix resin with HATU activation using a fully automatic flow-based peptide synthesizer[53]. Amide bond formation was effected in 8 s, and Fmoc groups were removed in 8 s with 20% (*v/v*) piperidine in DMF. Overall cycle times were about 40 s. After completion of fast-flow synthesis, the resins were washed with DCM (5×) and dried under reduced pressure.

Solid-phase synthesis of combinatorial peptide libraries.—

Libraries 1–5 were typically synthesized on Tentagel M NH_2 resin beads (30 µm, 0.22 mmol g^{-1}, Rapp Polymere) at a scale of 0.5 g of resin (~20×10^6 beads) using split and pool. Fixed regions were synthesized using manual SPPS or automated fast-flow synthesis. For each randomized residue, the resin was split equally among separate Torviq syringes and, for each coupling cycle, Fmoc-protected amino acids (5 equivalents with regard to resin substitution), HATU

(4.75 equivalents, 0.38 M solution), and DIEA (25 equivalents) were added for 30 min. The resin was then washed (5×) with DMF and pooled then deprotected (2×) with 20% (*v/v*) piperidine in DMF and finally washed (5×) with DMF to conclude the split and pool cycle. After synthesis completion, the resins were washed with DCM (5×) and dried under reduced pressure then cleaved and purified using RP-HPLC.

Peptide cleavage and deprotection.—Peptides were cleaved from the resin and side chains were simultaneously deprotected by treatment with 2.5% (v/v) 1,2-ethanedithiol (EDT), 5% (v/v) water, 5% (v/v) phenol, 5% (v/v) thioanisole in neat trifluoro acetic acid (TFA) for 8 min at 60 °C; 6 ml of cleavage cocktail was used for 0.1 mmol of peptide. The resulting solution was triturated and washed with cold ether (prechilled in −80 °C freezer) for linear peptides. In the case of macrocyclic peptides, the resulting solution was triturated and washed with cold ether/cold cyclohexane (50:50) (prechilled in −80 °C freezer). The trituration was repeated a total of three times. The obtained solids were dissolved in water/acetonitrile (50:50) and lyophilized.

Perfluoroarylsulfone macrocyclization.—A 50-ml conical tube was charged with peptide (10 ml, 1.25 mM stock solution in DMF) and DIEA solution (5 ml, 20 equivalents, 50 mM stock solution in DMF) was added[8]. The resulting mixture was capped and vortexed for 10 s. Then, perfluoroarylsulfone[3] (10 ml, 1.25 equivalents, 1.56 mM stock solution in DMF) was added. The resulting reaction mixture was capped, vortexed for 10 s, and left overnight at room temperature. DMF was removed under reduced pressure and the obtained residue was dissolved in a water/acetonitrile mixture with 0.1% TFA, filtered, then subjected to RP-HPLC purification.

Perfluoroarylsulfone macrocycle excision for compound 116.

Direct excision.: To crude **116** (1 μg, 5 μM) in 100 μl of 200 mM CAPS buffer was added 2-mercaptoethanol at a final concentration of 50 mM and pH was adjusted to 10. After vortexing, the mixture was left for 2 h at room temperature and analyzed by LC–MS (Supplementary Fig. 8).

After affinity selection.: First, 116 (100 ng, 500 nM) was added to MDM2 (20 μg, 8.6 μM) in 100 μl final volume of mobile phase supplemented with L-arginine at pH 7.5. The solution was left to stand for 1 h at room temperature before size exclusion chromatography. To the collected protein fraction was added CAPS and 2-mercaptoethanol to a final concentration of 200 mM and 50 mM, respectively, at pH 10 and the mixture was analyzed by LC–MS.

RCM macrocyclization.—RCM was performed on the peptide while still on the solid support[6,54]. An Eppendorf tube was charged with peptidyl resin (30 μmol) to which was added Hoveyda–Grubbs second-generation catalyst in 1,2-dichloroethane (1 ml of a 6-mM freshly prepared solution, 20 mol% with respect to resin substitution), under slow nitrogen bubbling and gentle agitation for 2 h at 50 °C. Completeness of the RCM reaction was monitored by LC–MS. On completion, resin-bound peptide was washed (5×) with DMF and with DCM (5×) and dried under vacuum.

Peptide labeling with biotin.—Peptide labeling with D-biotin was performed on the resin-bound protected peptides by treating the resin either with a solution of Biotin-PEG_4-NHS (ChemPep, 2 equivalents) and DIEA (4 equivalents) dissolved in DMF for 6 h at room temperature, or with a solution of D-biotin (10 equivalents), HATU (9.5 equivalents, 0.38-M solution), and DIEA (50 equivalents) in DMF for 20 min at room temperature. On completion, the resin was washed with DMF (5×) and DCM (5×) and dried under reduced pressure.

Peptide labeling with FITC.—Peptide labeling with FITC was performed on the resin-bound protected peptides by treating the N-terminal β-alanine-containing resin with a solution of fluorescein isothiocyanate isomer I (Chem-Impex International, 6 equivalents) and DIEA (10 equivalents) dissolved in DMF for 3 h at room temperature in the dark. On completion of the reaction, resin was washed with DMF (5×) and DCM (5×) and finally dried under reduced pressure.

Peptide and library oxidative folding.—Single miniproteins and library 5 were folded in the same conditions. Typically, to 1–2 mg of crude material was added 50 µl of 20× dissolving buffer (6 M guanidine hydrochloride, 5 mM tris(2-carboxyethyl) phosphine (TCEP) hydrochloride, 50 mM Tris, pH 7.7). The obtained suspension was thoroughly vortexed and left to stand for a few minutes before dilution in 950 µl of folding buffer (2 mM cystine, 2 mM cysteine, 50 mM Tris, pH 7.7). The thus-obtained solution was thoroughly stirred overnight in the library case or for a few hours under LC–MS monitoring for single miniproteins. The mixture was either filtered using solid-phase extraction in the library case or filtered using a 0.22-µm nylon filter followed by RP-HPLC purification for single miniproteins.

Miniprotein backbone cleavage via diol oxidation.

Cleavage after selection of 115.: **115** (4 µg, 13 µM) was mixed with trypsin (40 µg, 17.2 µM) in 100 µl of mobile phase and, after 1 h at room temperature, the binding mixture was subjected to size exclusion chromatography (Supplementary Fig. 9). Protein fraction was collected and solid-phase extracted using Pierce C-18 spin columns (Thermo Fisher) to remove trypsin. **115** was selectively eluted by 70:30 water/acetonitrile (50 µl with 0.2% TFA). The eluate was then diluted to 100 µl using Tris buffer (100 mM at pH 8.5) and solid urea was added (36 mg, ~6 M final concentration). Then, a freshly prepared solution of DTT (0.5 M in 50 mM Tris, pH 8.5) was added to a final concentration of 5 mM for 15 min at room temperature followed by addition of freshly prepared iodoacetamide solution (0.28 M in 50 mM Tris, pH 8.5) to a final concentration of 15 mM, and the mixture was kept in the dark for 30 min at room temperature. Reduced and alkylated **115** was desalted using solid-phase extraction and eluted with 70:30 water/acetonitrile (50 µl with 0.2% TFA). Sodium periodate (50 µl of a 2-mM stock solution) in 200 mM sodium acetate buffer at pH 5.5 was added and the resulting cleavage mixture was incubated at room temperature for 45 min. Finally, this mixture was quenched with 50% glycerol solution (2 µl) and freshly prepared methoxyamine (2 µl of a 0.5 M stock solution) in 100 mM Tris buffer and analyzed by LC–MS.

78 cleavage after selection. **78** (30 ng, 76 nM) was added to MDM2 (20 μg, 8.6 μM) in 100 μl final volume of mobile phase supplemented with L-arginine pH 7.5. After 1 h at room temperature, the binding mixture was subjected to size exclusion chromatography (Supplementary Fig. 25). Solid sodium periodate was added to the protein fraction (30 mM final concentration) and incubation for 45 min at 37 °C followed by glycerol quench and addition of methoxyamine hydrochloride (30 mM final concentration) afforded MDM2 binding peptide.

Cleavage after selection from library 5.: Crude folded library 5 (1.5 μg, ~3.75 μM) was added to MDM2 (20 μg, 8.6 μM) in 100 μl final volume of mobile phase supplemented with L-arginine pH 7.5 (Supplementary Fig. 26). After 1 h at room temperature, the binding mixture was subjected to size exclusion chromatography. Solid sodium periodate was added to the protein fraction (30 mM final concentration) and incubation for 45 min at 37 °C followed by glycerol quench and addition of methoxyamine hydrochloride (30 mM final concentration) afforded MDM2 binding peptides.

OBOC library 3 screening.—Direct staining: focused and redundant (redundancy > 300) peptide library with the same design as library 3 (Fig. 3a) was synthesized on attenuated Tentagel resin (OBOC library 3, 5% loading, 10 μmol g^{-1}, 90 μm beads functionalized with PAM linker). Then, 5 mg of the peptidyl resin was dispersed in 1 ml of PBS for 10 min then washed 1 more time with PBS. The resin was then blocked for 1 h in 0.1% tween and 10 mg ml^{-1} BSA in PBS (10× blocking buffer) and then incubated with 0.25 ml of MDM2-SA-AP complex at different concentrations in 1× blocking buffer supplemented with arginine for 1 h at room temperature. The resin was then rapidly washed 3× (1 ml each) with PBS, 1× with 1 ml TBS buffer (2.5 mM Tris-HCl, 13.7 mM NaCl, 0.27 mM KCl pH 8.0), and finally beads were placed into polystyrene Petri dishes (10 cm diameter). Each dish then received the alkaline phosphatase substrate 5-bromo-4-chloro-3-indoyl phosphate (BCIP) in BCIP buffer (0.1 M Tris-HCl, 0.1 M NaCl, and 2.34 mM $MgCl_2$ pH 8.8) to develop color at room temperature.

Indirect staining: 5 mg of focused and redundant OBOC library 3 (5% loading, 10 μmol g^{-1}, 90 μm beads functionalized with PAM linker) was dispersed in 1 ml of 10× blocking buffer (0.1% tween and 10 mg ml^{-1} BSA, 50 mM Tris-HCl). The resin was kept on a rotary vertical mixer for 1 h and then incubated with 0.2 ml MDM2-Biotin at 30 nM concentration in 1× blocking buffer supplemented with arginine for 1 h at room temperature. The resin was then washed 3× (50 ml each) with 1× blocking buffer, then incubated with 0.6 ml of 5 nM SA-AP in 1× blocking buffer for 1 h at room temperature. The resin was then washed 3× (1 ml ea.) with PBS and 1 time with 1 ml of TBS buffer (2.5 mM Tris-HCl, 13.7 mM NaCl, 0.27 mM KCl pH 8.0), and finally beads were placed into polystyrene Petri dishes (10 cm diameter). Each dish then received the alkaline phosphatase substrate BCIP in BCIP buffer (0.1 M Tris-HCl, 0.1 M NaCl, and 2.34 mM MgCl2 pH 8.8) to develop color at room temperature.

RP-HPLC purification.—Crude peptides were dissolved in a water/acetonitrile mixture with 0.1% TFA and purified by semipreparative RP-HPLC using a Waters 600 HPLC system (Agilent Zorbax SB-C3 column: 9.4 × 250 mm^2, 5 μm; or Agilent Zorbax SB C18 column:

9.4 × 250 mm^2, 5 μm; or Agilent Zorbax SB-C3 column: 21.2 × 250 mm^2, 7 μm). HPLC fractions containing pure product were confirmed by LC–MS analysis, combined, and lyophilized.

LC–MS analysis of synthesized peptides.—Samples were analyzed by LC–MS (Agilent 6520 or 6550 ESI-Q-TOF) using Agilent Zorbax 300 SB-C3 (2.1×150 mm^2, 5 μm particle size) or Agilent Poroshell 300 SB-C3 (1.0×75 mm^2, 5-μm particle size) analytical columns. Mobile phases were: 0.1% formic acid in water (solvent A) and 0.1% formic acid in acetonitrile (solvent B). Total ion chromatograms and integrated MS over the main peak are provided (see Supplementary Note 2). Alternatively, LC-UV chromatograms (214 nm detection using 6520 ESI-Q-TOF) and integrated MS over the main peak are provided for poorly ionizing compounds.

BLI-based validation assays.

Kinetic binding assay with immobilized peptide.—In vitro binding assays[8] were performed using Fortebio Octet RED96 BLI system (Octet RED96), typically at 30 °C and 1,000 r.p.m. Briefly, streptavidin (SA) tips were dipped in 200 μl of biotinylated peptide solution (2.5 μM in PBS with 0.05% tween) for the loading step. The tips loaded with peptide were then sampled with SUMO-$^{25–109}$MDM2 or SUMO-C-CA at various concentrations in PBS with 0.05% tween to obtain the association curve. Buffer-only and protein-only conditions (at the highest sampled protein concentration) were used as references for background substraction. After association, the tips were dipped back into PBS and 0.05% tween to obtain the dissociation curve. The association and dissociation curves were fitted with Fortebio Biosystems using 4 experimental conditions ($n = 4$, global fitting algorithm, binding model 1:1) to obtain the dissociation constant (K_d, see Supplementary Note 1). When biotinylated proteins were assayed, the binding assay was modified to include a quenching step after biotinylated peptide immobilization. Tips were dipped in a (D)-Biotin solution (10 μM) to saturate streptavidin sites before washing and association. This treatment abrogated binding of biotinylated proteins to a reference streptavidin sensor.

In-solution competition assay.

A competition binding assay[30,50] was performed as described below using the same BLI system to estimate the binding affinity of N terminus free or acetylated peptides and miniprotein binders of SUMO-$^{25–109}$MDM2.

Calibration curve.—Streptavidin sensors were soaked in competition buffer (PBS supplemented with 0.05% Tween-20, and L-arginine pH 7.5) for 10 min at 30 °C. Modified $^{15–29}$p53 peptide with an N-terminal Gly-Ser linker (sequence: $(Gly\text{-}Ser)_6$-Ser-Gln-Glu-Thr-Phe-Ser-Asp-Leu-Trp-Lys-Leu-Leu-Pro-Glu-Asn) was fast-flow synthesized and labeled with D-biotin on its N terminus. The thus-obtained biotinylated **118** was loaded on the streptavidin tip for 10 min. Then, serial dilutions of SUMO-$^{2515–109}$MDM2 in competition buffer were analyzed for binding, typically at 30 °C and 1,000 r.p.m. A calibration curve corresponding to binding response (in nm) = f(free [MDM2] in nM) was generated using GraphPad Prism 7 software using nonlinear regression analysis.

Competition assay.—Various concentrations of peptides and miniprotein binders were incubated in wells with MDM2 protein in competition buffer at room temperature for 30 min. Meanwhile, streptavidin sensors were soaked in competition buffer for 10 min at 30 °C. Peptide **118** was immobilized on the streptavidin sensor surface and the association and dissociation curves of MDM2 preincubated samples were then analyzed at 30 °C and 1,000 r.p.m. Based on the binding response (nm) values, the concentration of 'free' MDM2 was interpolated for each sample using the calibration curve. Nonlinear regression analysis was performed using GraphPad Prism 6 software to estimate the K_d value based on the equation: K_d = [peptide][MDM2]/[complex]. We used the following equation to generate fitted curves: $[MDM2] = 0.5 \times [(b\text{-}K_d\text{-}[X]) + (([X] + K_d\text{-}b)^2 + 4b \times K_d)^{(0.5)}]$, where [MDM2] is 'free' MDM2 in nM, X is the peptide inhibitor in nM, K_d is the dissociation constant, and b is ymax (see Supplementary Note 1).

Cell-based assays.

Confocal imaging.—SJSA-1 cells were cultured in 24-well plates containing cover slips until they reached 80% confluency[8]. Appropriate amounts of peptides were dissolved in RPMI-1640 supplemented with 10% serum and 1% Pen-Strep and were added to the cells to a final concentration of 10 μM (0.1% DMSO). Cells were incubated with the samples for 4 h at 37 °C and 5% CO_2. After incubation, cells were washed (2×) with HBSS and 1 more time with PBS then fixed with 4% formaldehyde (Alfa Aesar) in Dulbecco's phosphate-buffered saline (DPBS) for 10 min. Cells were then washed (2×) with PBS and stained with 5 μg ml^{-1} Wheat Germ Agglutinin 633 conjugate (WGA, Thermo Fisher) in PBS for 20 min. Finally, cells were washed (2×) with PBS and the cover slips were transferred to microscope slides and imaged using scan confocal microscope Leica DMRXE.

Flow cytometry.—SJSA-1 cells were cultured in 24-well plates until they reached 80% confluency[55]. Appropriate amounts of peptides dissolved in RPMI-1640 medium supplemented with 10% FBS and 1% Pen-Strep were added to cells to a final concentration of 10 μM and incubated for 4 h at 37 °C and 5% CO_2. Supernatant was removed and trypsin-EDTA 0.25% (0.5 ml) was added to cells and incubated for 10 min at 37 °C and 5% CO_2. After incubation, cells were recovered by pipetting then transferred to Eppendorf tubes and spun down at 2,200 r.p.m. for 3 min. The pellets were washed 3 times with PBS then resuspended in PBS with 2% FBS (*v/v*) before filtration using Cell Strainer caps. Cells were finally treated with trypan blue (Thermo Fisher) and the fluorescence of individual cells was measured on a BD LSRII Flow Cytometer (wavelengths were 488 nm for excitation and 525 nm for detection and 10,000 events were recorded for every experimental condition). Results were analyzed using FlowJo software.

Western blot analysis of p53 activation by macrocyclic inhibitors.—SJSA-1 cells were seeded in 6-well plates at a cell density of 350×10^3 cells per well in RPMI-1640 medium supplemented with 10% serum and 1% Pen-Strep and incubated overnight at 37 °C and 5% CO_2 (see refs. [26,41,48]). The next day, cells were treated with compounds and controls at 10 μM for 24 h. Then, cells were harvested and their pellets washed (2×) with PBS and lysed in 100 μl of RIPA buffer supplemented with Roche protease inhibitor cocktail on ice for 30 min. The lysates were clarified by brief centrifugation at 4 °C and total protein

concentration was determined using the Bio-Rad DC protein assay. Aliquots of the cell lysates were run on 12% Tris-Glycine polyacrylamide gels (Invitrogen). After transfer using Trans-Blot Turbo Transfer system (Bio-rad), PVDF membrane was blocked at room temperature for 2 h with LI-COR blocking buffer. Based on molecular weight, the membrane was cut into 3 separate parts and each part was incubated respectively with anti-MDM2 (mouse, SMP14: sc-965, Santa Cruz Biotechnology), anti-p21 (mouse, F-5: sc-6246, Santa Cruz Biotechnology), and anti-GAPDH (rabbit, GAPDH (D16H11) XP, Cell Signaling Technology) antibodies in tris-buffered saline supplemented with Tween 20 (TBST) overnight at 4 °C. The membranes were washed and incubated with the appropriate secondary antibodies in TBST for 1 h at room temperature, washed again, then imaged with the LI-COR Odyssey infrared imaging system.

Cell viability assays.—SJSA-1 cells were plated in 96-well plates in RPMI-1640 containing 10% FBS and 1% Pen-Strep and treated with the indicated concentrations of peptide[26,41,48]. Peptide stocks were diluted into RPMI-1640 containing 10% FBS and 1% Pen-Strep to achieve 2× working individual stock solutions that were thoroughly mixed then diluted into the treatment wells. After 4 d, cell viability was assayed using CellTiter 96 AQueous One Solution Cell Proliferation reagent (MTS). Data were normalized to untreated controls and analyzed using Prism software (GraphPad).

Statistics and reproducibility.

No statistical tests were used in this study. As applicable, error bars are defined in figure legends, and for all representative results numbers of times experiments were repeated and types of replicates are specified.

Reporting Summary.

Further information on research design is available in the Nature Research Reporting Summary linked to this article.

Data availability

The authors declare that all data supporting the findings of this study are available within the manuscript, its Supplementary Information, and Supplementary Notes.

Supplementary Material

Refer to Web version on PubMed Central for supplementary material.

Acknowledgements

The Bettencourt Schueller Foundation is gratefully acknowledged for postdoctoral support to F.T. The Human Frontier Science Program Organization is thanked for a cross-disciplinary fellowship (LT000745/2014-C) to F.T. This work was supported in part by Servier, the Defense Advanced Research Projects Agency (award no. 023504-001 to B.L.P.), the NIH National Institute of General Medical Sciences (grant no. 5-R01-GM110535 to B.L.P.), a Bristol-Myers Squibb unrestricted grant in Synthetic Organic Chemistry (B.L.P.), and a Novartis Early Career Award (B.L.P). F. Lefoulon (Servier) is thankfully acknowledged for his suggestions and comments on the manuscript. FACS experiments were performed at the MIT Koch Institute Flow Cytometry Core. The authors thank the Biophysical Instrumentation Facility at MIT for providing access to the Octet Bio-Layer Interferometry System (NIH S10OD016326) and D. Pheasant for her technical assistance and B. Dass (Pall Fortebio) for his help with data

analysis. We gratefully acknowledge A. Rabideau for peptide synthesis and characterization training, A. Quartararo for help with the Orbitrap LC–MS instrument, and A. Vinogradov and M. Simon for scientific discussions.

References

1. Wells JA & McClendon CL Reaching for high-hanging fruit in drug discovery at protein–protein interfaces. Nature 450, 1001–1009 (2007). [PubMed: 18075579]
2. Petta I, Lievens S, Libert C, Tavernier J & De Bosscher K Modulation of protein–protein interactions for the development of novel therapeutics. Mol. Ther 24, 707–718 (2016). [PubMed: 26675501]
3. Modell AE, Blosser SL & Arora PS Systematic targeting of protein–protein interactions. Trends Pharmacol. Sci 37, 702–713 (2016). [PubMed: 27267699]
4. Pelay-Gimeno M, Glas A, Koch O & Grossmann TN Structure-based design of inhibitors of protein–protein interactions: mimicking peptide binding epitopes. Angew. Chem. Int. Ed. Engl 54, 8896–8927 (2015). [PubMed: 26119925]
5. Valeur E et al. New modalities for challenging targets in drug discovery. Angew. Chem. Int. Ed. Engl 56, 10294–10323 (2017). [PubMed: 28186380]
6. Grossmann TN et al. Inhibition of oncogenic Wnt signaling through direct targeting of β-catenin. Proc. Natl Acad. Sci. USA 109, 17942–17947 (2012). [PubMed: 23071338]
7. Spokoyny AM et al. A perfluoroaryl-cysteine SNAr chemistry approach to unprotected peptide stapling. J. Am. Chem. Soc 135, 5946–5949 (2013). [PubMed: 23560559]
8. Lautrette G, Touti F, Lee HG, Dai P & Pentelute BL Nitrogen arylation for macrocyclization of unprotected peptides. J. Am. Chem. Soc 138, 8340–8343 (2016). [PubMed: 27332147]
9. Renfrew PD, Choi EJ, Bonneau R & Kuhlman B Incorporation of noncanonical amino acids into Rosetta and use in computational protein–peptide interface design. PLoS One 7, 1–15 (2012).
10. Drew K et al. Adding diverse noncanonical backbones to Rosetta: enabling peptidomimetic design. PLoS One 8, 1–17 (2013).
11. Rognan D, Scapozza L & Folkers G & Daser A Rational design of nonnatural peptides as high-affinity ligands for the HLA-B*2705 human leukocyte antigen. Proc. Natl Acad. Sci. USA 92, 753–757 (1995).. [PubMed: 7846047]
12. Zhan C et al. An ultrahigh affinity D-peptide antagonist Of MDM2. J. Med. Chem 55, 6237–6241 (2012). [PubMed: 22694121]
13. Zhou H-B et al. Structure-based design of high-affinity macrocyclic peptidomimetics to block the menin-MLL1 protein–protein interaction. J. Med. Chem 1, 1113–1123 (2012).
14. Kritzer JA, Luedtke NW, Harker EA & Schepartz A A rapid library screen for tailoring β-peptide structure and function. J. Am. Chem. Soc 127, 14584–14585 (2005). [PubMed: 16231906]
15. Upadhyaya P et al. Inhibition of Ras signaling by blocking Ras-effector interactions with cyclic peptides. Angew. Chem. Int. Ed. Engl 54, 7602–7606 (2015). [PubMed: 25950772]
16. Annis DA, Nazef N, Chuang CC, Scott MP & Nash HM A general technique to rank protein–ligand binding affinities and determine allosteric versus direct binding site competition in compound mixtures. J. Am. Chem. Soc 126, 15495–15503 (2004). [PubMed: 15563178]
17. Zuckermann RN, Kerr JM, Siani MA, Banville SC & Santi DV Identification of highest-affinity ligands by affinity selection from equimolar peptide mixtures generated by robotic synthesis. Proc. Natl Acad. Sci. USA 89, 4505–4509 (1992). [PubMed: 1584783]
18. Annis DA, Nickbarg E, Yang X, Ziebell MR & Whitehurst CE Affinity selection-mass spectrometry screening techniques for small molecule drug discovery. Curr. Opin. Chem. Biol 11, 518–526 (2007). [PubMed: 17931956]
19. Comess KM et al. An ultraefficient affinity-based high-throughout screening process: application to bacterial cell wall biosynthesis enzyme MurF. J. Biomol. Screen 11, 743–754 (2006). [PubMed: 16973923]
20. Dunayevskiy YM, Lai J-J, Quinn C, Talley F & Vouros P Mass spectrometric identification of ligands selected from combinatorial libraries using gel filtration. Rapid Commun. Mass Spectrom 11, 1178–1184 (1997).

21. Huyer G et al. Affinity selection from peptide libraries to determine substrate specificity of protein tyrosine phosphatases. Anal. Biochem 258, 19–30 (1998). [PubMed: 9527843]
22. Vinogradov AA et al. Library design-facilitated high-throughput sequencing of synthetic peptide libraries. ACS Comb. Sci 19, 694–701 (2017). [PubMed: 28892357]
23. Muckenschnabel I, Falchetto R, Mayr LM & Filipuzzi I SpeedScreen: label-free liquid chromatography-mass spectrometry-based high-throughput screening for the discovery of orphan protein ligands. Anal. Biochem 324, 241–249 (2004). [PubMed: 14690688]
24. O'Connell TN, Ramsay J, Rieth SF, Shapiro MJ & Stroh JG Solution-based indirect affinity selection mass spectrometry—a general tool for high-throughput screening of pharmaceutical compound libraries. Anal. Chem 86, 7413–7420 (2014). [PubMed: 25033415]
25. Kussie PH et al. Structure of the MDM2 oncoprotein bound to the p53 tumor suppressor transactivation domain. Science 274, 948–953 (1996). [PubMed: 8875929]
26. Vassilev LT et al. In vivo activation of the p53 pathway by small-molecule antagonists of MDM2. Science 303, 844–848 (2004). [PubMed: 14704432]
27. Li C et al. Systematic mutational analysis of peptide inhibition of the p53–MDM2/MDMX interactions. J. Mol. Biol 398, 200–213 (2010). [PubMed: 20226197]
28. Böttger A et al. Molecular characterization of the hdm2–p53 interaction. J. Mol. Biol 269, 744–756 (1997). [PubMed: 9223638]
29. Phan J et al. Structure-based design of high affinity peptides inhibiting the interaction of p53 with MDM2 and MDMX. J. Biol. Chem 285, 2174–2183 (2010). [PubMed: 19910468]
30. Pazgier M et al. Structural basis for high-affinity peptide inhibition of p53 interactions with MDM2 and MDMX. Proc. Natl Acad. Sci. USA 106, 4665–4670 (2009). [PubMed: 19255450]
31. Liu R, Li X & Lam KS Combinatorial chemistry in drug discovery. Curr. Opin. Chem. Biol 38, 117–126 (2017). [PubMed: 28494316]
32. Ferrer M et al. Selection of gp41-mediated HIV-1 cell entry inhibitors from biased combinatorial libraries of non-natural binding elements. Nat. Struct. Biol 6, 953–960 (1999). [PubMed: 10504731]
33. Wang X, Peng L, Liu R, Xu B & Lam KS Applications of topologically segregated bilayer beads in combinatorial libraries. J. Pept. Res 65, 130–138 (2005). [PubMed: 15686543]
34. Lam KS et al. A new type of synthetic peptide library for identifying ligand-binding activity. Nature 354, 82–84 (1991). [PubMed: 1944576]
35. Lam KS & Lebl M Selectide technology: bead-binding screening. Methods 6, 372–380 (1994).
36. Chen CL, Strop P, Lebl M & Lam KS Synthesis of libraries for bead-binding screening. Methods Enzymol. 267, 211–219 (1996). [PubMed: 8743318]
37. Alluri PG, Reddy MM, Bachhawat-Sikder K, Olivos HJ & Kodadek T Isolation of protein ligands from large peptoid libraries. J. Am. Chem. Soc 125, 13995–14004 (2003). [PubMed: 14611236]
38. Reddy MM, Bachhawat-Sikder K & Kodadek T Transformation of low-affinity lead compounds into high-affinity protein capture agents. Chem. Biol 11, 1127–1137 (2004). [PubMed: 15324814]
39. Zondlo SC, Lee AE & Zondlo NJ Determinants of specificity of MDM2 for the activation domains of p53 and p65: Proline27 disrupts the MDM2-binding motif of p53. Biochemistry 45, 11945–11957 (2006). [PubMed: 17002294]
40. Furman JL, Chiu M & Hunter MJ Early engineering approaches to improve peptide developability and manufacturability. AAPS J 17, 111–120 (2015). [PubMed: 25338742]
41. Chang YS et al. Stapled α-helical peptide drug development: a potent dual inhibitor of MDM2 and MDMX for p53-dependent cancer therapy. Proc. Natl Acad. Sci. USA 110, E3445–E3454 (2013). [PubMed: 23946421]
42. Adamson CS & Freed EO Anti-HIV-1 therapeutics: from FDA-approved drugs to hypothetical future targets. Mol. Interv 9, 70–74 (2009). [PubMed: 19401538]
43. Bartonova V et al. Residues in the HIV-1 capsid assembly inhibitor binding site are essential for maintaining the assembly-competent quaternary structure of the capsid protein. J. Biol. Chem 283, 32024–32033 (2008). [PubMed: 18772135]

44. Ternois F, Sticht J, Duquerroy S, Kräusslich HG & Rey FA The HIV-1 capsid protein C-terminal domain in complex with a virus assembly inhibitor. Nat. Struct. Mol. Biol 12, 678–682 (2005). [PubMed: 16041386]
45. Heitz a, Le-Nguyen D & Chiche L Min-21 and min-23, the smallest peptides that fold like a cystine-stabilized β-sheet motif: design, solution structure, and thermal stability. Biochemistry 38, 10615–10625 (1999). [PubMed: 10441159]
46. Celie PHN et al. UV-induced ligand exchange in MHC class I protein crystals. J. Am. Chem. Soc 131, 12298–12304 (2009). [PubMed: 19655750]
47. Zhang H et al. A cell-penetrating helical peptide as a potential HIV-1 inhibitor. J. Mol. Biol 378, 565–580 (2008). [PubMed: 18374356]
48. Wachter F et al. Mechanistic validation of a clinical lead stapled peptide that reactivates p53 by dual HDM2 and HDMX targeting. Oncogene 36, 2184–2190 (2017). [PubMed: 27721413]
49. Goodnow RA, Dumelin CE & Keefe AD DNA-encoded chemistry: enabling the deeper sampling of chemical space. Nat. Rev. Drug Discov 16, 131–147 (2017). [PubMed: 27932801]
50. Rabideau AE, Liao X & Pentelute BL Delivery of mirror image polypeptides into cells. Chem. Sci 6, 648–653 (2015). [PubMed: 28706631]
51. Vinogradov AA, Choo ZN, Totaro KA & Pentelute BL Macrocyclization of unprotected peptide isocyanates. Org. Lett 18, 1226–1229 (2016). [PubMed: 26948900]
52. Rodenko B et al. Class I major histocompatibility complexes loaded by a periodate trigger. J. Am. Chem. Soc 131, 12305–12313 (2009). [PubMed: 19655751]
53. Mijalis AJ et al. A fully automated flow-based approach for accelerated peptide synthesis. Nat. Chem. Biol 13, 464–466 (2017). [PubMed: 28244989]
54. Kim Y-W, Grossmann TN & Verdine GL Synthesis of all-hydrocarbon stapled α-helical peptides by ring-closing olefin metathesis. Nat. Protoc 6, 761 (2011). [PubMed: 21637196]
55. Illien F et al. Quantitative fluorescence spectroscopy and flow cytometry analyses of cell-penetrating peptides internalization pathways: optimization, pitfalls, comparison with mass spectrometry quantification. Sci. Rep 6, 1–13 (2016). [PubMed: 28442746]

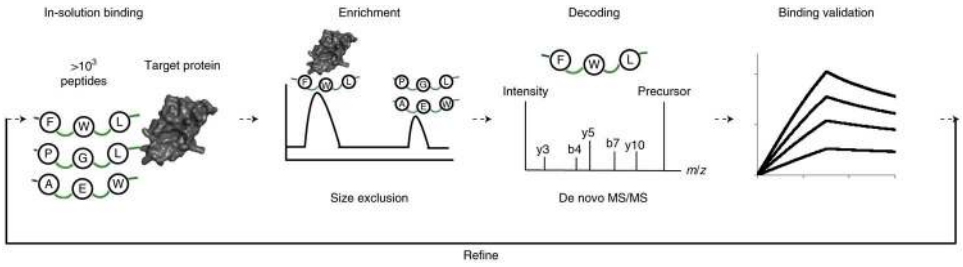

Fig. 1. Affinity selection platform for the maturation of known peptide binders.

Synthetic peptide libraries are prepared by randomizing select residues within the sequence of a known peptide binder using the split and pool technique. These focused libraries are then bound to a protein target in solution where binding conditions can be tuned. The binding mixture is subjected to HPSEC allowing for high resolution of protein–binder complexes from unbound library members. The breakthrough fraction (or protein fraction) is then directly analyzed in the case of linear binders or subjected to chemical conditions to linearize binding sequences before LC–MS/MS analysis. The decoded sequences are then synthesized and chemically modified to allow for validation using binding or functional assays.

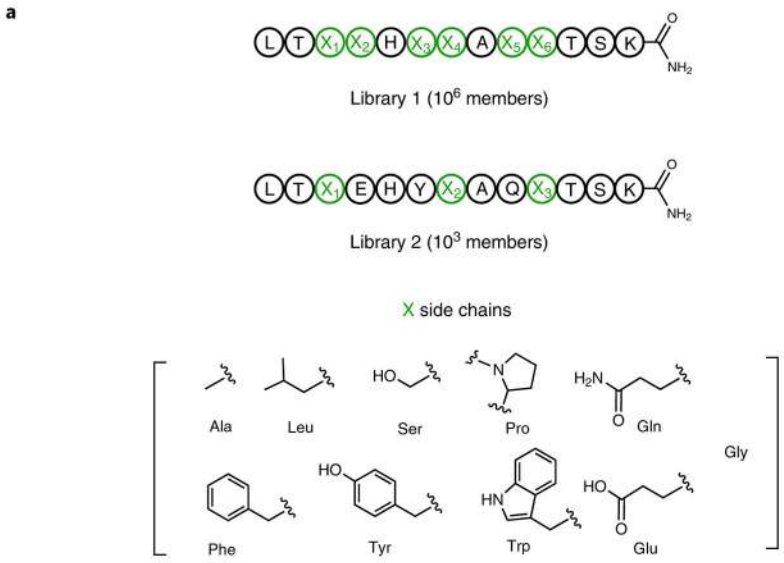

b

															K_d MDM2 (nM)
2	Bio-$(PEG)_4$-	Leu	Thr	*Phe*	*Gln*	His	*Phe*	*Trp*	Ala	*Glu*	*Leu*	Thr	Ser	Lys	-NH_2	45
3	Bio-$(PEG)_4$-	Leu	Thr	*Phe*	*Gln*	His	*Tyr*	*Trp*	Ala	*Glu*	*Leu*	Thr	Ser	Lys	-NH_2	62
4	Bio-$(PEG)_4$-	Leu	Thr	*Phe*	*Pro*	His	*Tyr*	*Trp*	Ala	*Glu*	*Leu*	Thr	Ser	Lys	-NH_2	80
5	Bio-$(PEG)_4$-	Leu	Thr	*Phe*	*Pro*	His	*Phe*	*Trp*	Ala	*Glu*	*Leu*	Thr	Ser	Lys	-NH_2	120

c

															K_d MDM2 (nM)
1		Leu	Thr	*Phe*	Glu	His	Tyr	*Trp*	Ala	Gln	*Leu*	Thr	Ser	Lys	-NH_2	25
6	Bio-$(PEG)_4$-	Leu	Thr	*Phe*	Glu	His	Tyr	*Trp*	Ala	Gln	*Phe*	Thr	Ser	Lys	-NH_2	36
7	Bio-$(PEG)_4$-	Leu	Thr	*Phe*	Glu	His	Tyr	*Trp*	Ala	Gln	*Leu*	Thr	Ser	Lys	-NH_2	47
8	Ac-	Leu	Thr	*Phe*	Glu	His	Tyr	*Trp*	Ala	Gln	*Tyr*	Thr	Ser	Lys	-NH_2	490
9	Ac-	Leu	Thr	*Tyr*	Glu	His	Tyr	*Trp*	Ala	Gln	*Leu*	Thr	Ser	Lys	-NH_2	2,500
10	Ac-	Leu	Thr	*Leu*	Glu	His	Tyr	*Trp*	Ala	Gln	*Leu*	Thr	Ser	Lys	-NH_2	8,700

Fig. 2. Affinity selection identifies hotspot residues for MDM2 binding.

a, Libraries designed to map hotspots for binding of pDI to $^{2515–109}$MDM2. Positions randomized using select canonical L-amino acids are shown in green. In library 1, both hotspot and adjacent positions were randomized; in library 2, only 'triad' hotspots were randomized. **b**, Validated MDM2 binders, identified by affinity selection from library 1. Binding constants were determined by kinetic binding assay using BLI (biotinylated compounds **2**–**5**). Residues corresponding to a varied position are in italic; residues not common to pDI are in green. **c**, Validated MDM2 binders, identified by affinity selection from library 2. Binding constants were determined by kinetic binding assay or competition assay (biotinylated compounds **6** and **7**; compound **1** and acetylated compounds **8**–**10**) using BLI. Residues corresponding to a varied position are in italic; residues not common to pDI are in green.

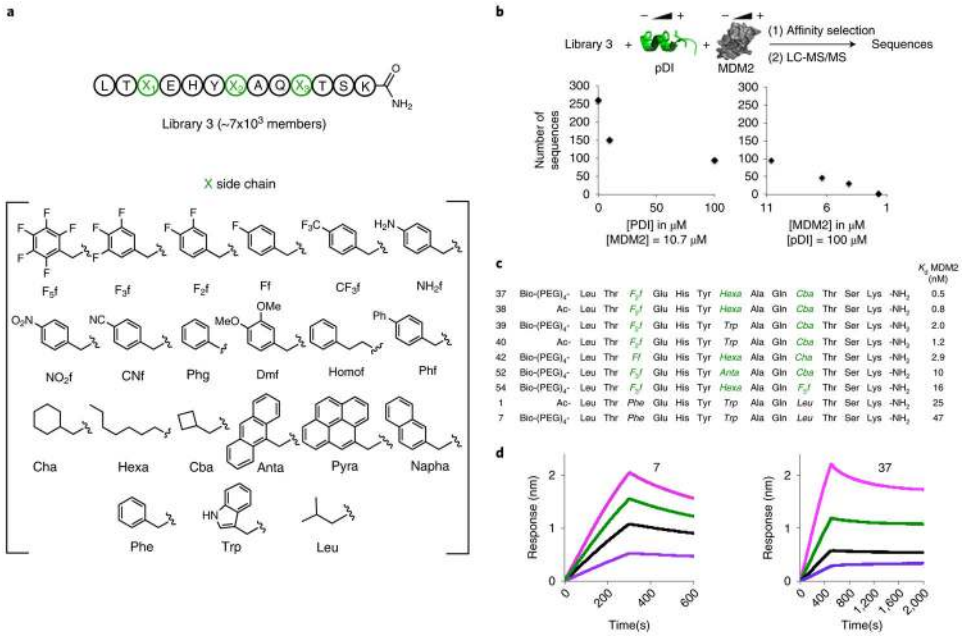

Fig. 3. Affinity selection identifies potent variants containing non-canonical amino acids.

a, Design of a non-canonical amino acid-containing library based on pDI. Hotspot positions (green) were randomized using select commercial L-configured non-canonical amino acids. **b**, Competitive selection conditions diminish the number of detected sequences. The number of detected variants is plotted as a function of affinity selection conditions (varying the concentrations of exogenous competitor (pDI) and MDM2). Maximal stringency was achieved at high-pDI (100 μM) and low-MDM2 concentrations (1.7 μM); in these conditions only 1 sequence from library 3 was de novo MS/MS sequenced. **c**, Select validated MDM2 binders, identified by affinity selection from library 3. Binding constants were determined by kinetic binding assay or competition assay using BLI. Residues corresponding to a varied position are in italic; residues not common to pDI are in green. **d**, Side-by-side comparison of BLI kinetic traces for **7** (left) and improved variant **37** (right). For **7**, traces correspond to MDM2 concentrations of 10 nM (purple), 20 nM (black), 30 nM (green), and 40 nM (magenta); determined kinetic parameters were $k_{on} = 2.1\times10^{4}M^{-1}s^{-1}$ and $k_{off} = 10^{-3}s^{-1}$. For **37**, traces correspond to MDM2 concentrations of 5 nM (purple), 10 nM (black), 20 nM (green), and 40 nM (magenta); determined kinetic parameters were $k_{on} = 6.1\times10^{4}M^{-1}s^{-1}$ and $k_{off} = 1.4\times10^{-5}s^{-1}$. For compounds **7** and **37**, 2 independent experiments were performed under analogous conditions, and gave similar results.

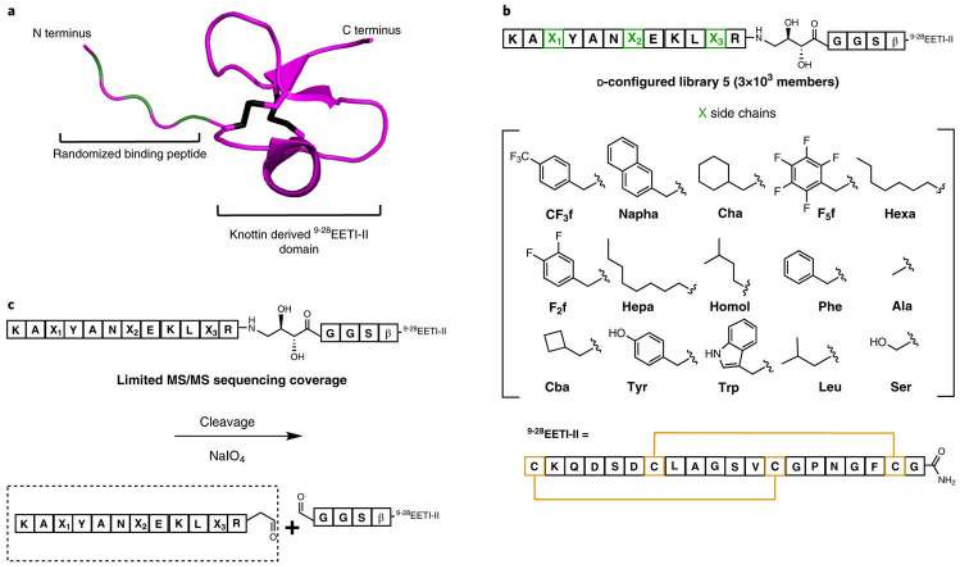

d

																		K_d MDM2 (nM)
68		Lys	Ala	*Trp*	Tyr	Ala	Asn	*Hexa*	Glu	Lys	Leu	*Homol*	Arg	Diol	Gly	Gly	Ser	β-Ala	9-28EETI-II	1
69		Lys	Ala	*Trp*	Tyr	Ala	Asn	*Hexa*	Glu	Lys	Leu	*Cha*	Arg	Diol	Gly	Gly	Ser	β-Ala	9-28EETI-II	4.5
70		Lys	Ala	*Trp*	Tyr	Ala	Asn	*Cha*	Glu	Lys	Leu	*Leu*	Arg	Diol	Gly	Gly	Ser	β-Ala	9-28EETI-II	6
71		Lys	Ala	*Trp*	Tyr	Ala	Asn	*Hexa*	Glu	Lys	Leu	*Hexa*	Arg	Diol	Gly	Gly	Ser	β-Ala	9-28EETI-II	10
72		Lys	Ala	*Trp*	Tyr	Ala	Asn	*Hexa*	Glu	Lys	Leu	*Trp*	Arg	Diol	Gly	Gly	Ser	β-Ala	9-28EETI-II	13
78		Lys	Ala	*Trp*	Tyr	Ala	Asn	*CF_3f*	Glu	Lys	Leu	*Leu*	Arg	Diol	Gly	Gly	Ser	β-Ala	9-28EETI-II	26
79	Ac-	Lys	Ala	*Trp*	Tyr	Ala	Asn	*CF_3f*	Glu	Lys	Leu	*Leu*	Arg							1.3

Fig. 4. Discovery of potent mirror image knottin derived peptide binders to MDM2.

a, Design of a high-molecular-weight, D-configured fusion peptide library. The scaffold was based on a D-configured minimal cystine knot domain derived from EETI-II, fused to a D-configured MDM2-binding peptide. Disulfide bridges are depicted in black; randomized positions are depicted in green, and fixed regions in magenta. **b**, Design of the varied portion of the cystine knot fusion library. Positions randomized using the indicated D-configured non-canonical amino acids are shown in green. **c**, Strategy for excising and sequencing the varied portion of the fusion construct. A diol amino acid was inserted between the cystine knot domain and the varied portion, to facilitate oxidative cleavage by periodate. **d**, Select cystine knot fusion-derived MDM2 binders, identified by affinity selection from library 5. Binding constants were determined by competition BLI assay. Residues corresponding to a varied position are in bold italic; residues not common to **78** are in green.

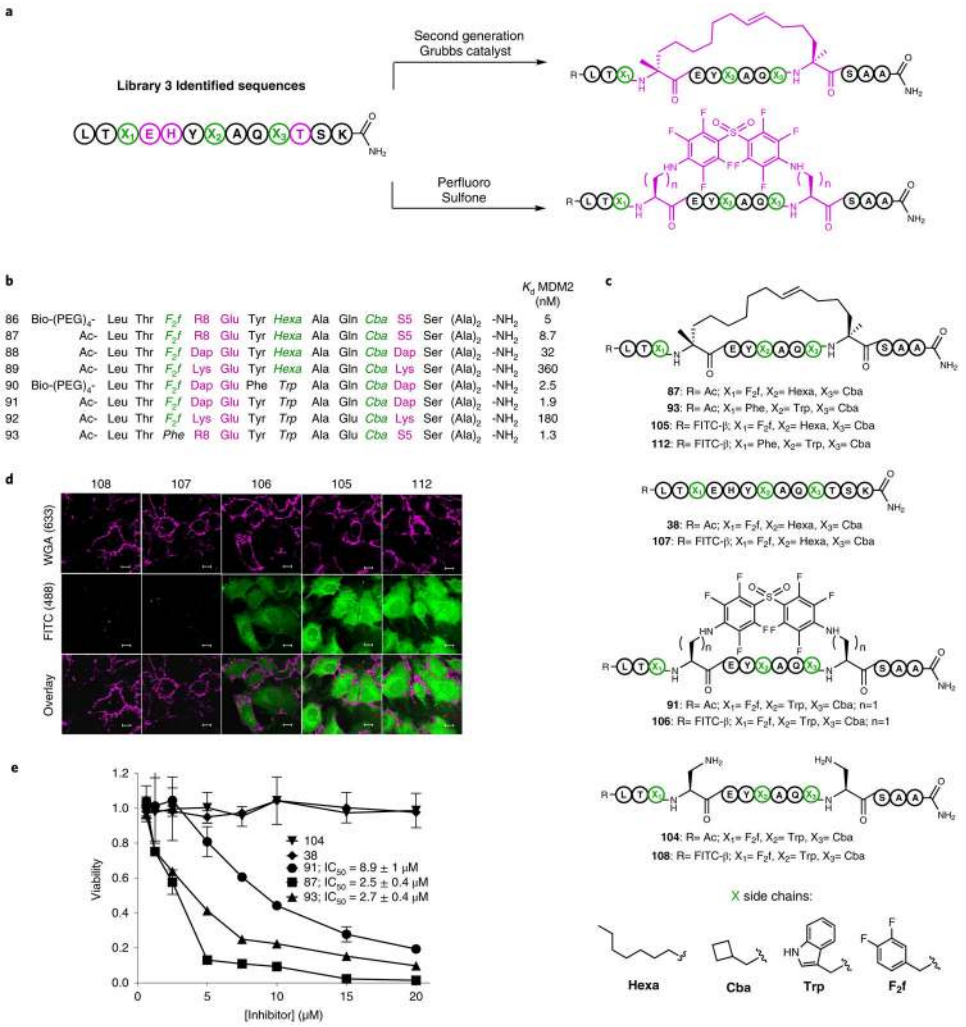

Fig. 5. Macrocyclic variants were cell penetrating and active against oncogenic cells overexpressing MDM2.

a, Select MDM2 binders identified from library 3 were macrocyclized for evaluation as MDM2 inhibitors (hotspots are in green). For each variant, His5 was mutated to Glu, to improve solubility (magenta). Glu4 and Thr11 (magenta) were replaced with the appropriate residues to facilitate *i* and *i* + 7 macrocyclization by either metathesis, lysine arylation, or diamino propionic acid arylation. **b**, Select macrocyclic products were evaluated for MDM2 binding. Biotinylated compounds (**86** and **90**) were evaluated for binding using BLI kinetic assay and acetylated compounds (**88**, **89**, **91**, and **92**) using competition assay. In magenta are represented residues modified to facilitate macrocyclization. Residues not common to pDI are in green. **c**, Molecular structures of macrocyclic MDM2 binders and linear controls selected for evaluation in cell assays. **d**, Penetration of MDM2-overexpressing SJSA-1 cells by macrocyclic MDM2 binders or linear controls was evaluated by confocal microscopy imaging (10 μM peptide, ×126 magnification). Cell membranes are colored in purple (WGA staining); fluorescence of FITC-labeled peptide is in green. This experiment was performed 1 time and cell penetration of compounds **105** and **106** was confirmed in an independent experiment with similar results. Scale bars (in white) represent 80 μm. **e**, Cell viability

responses of SJSA-1 cells to treatment with macrocyclic compounds and their controls. Macrocyclic binders **87** and **91** reduced cell viability in a dose-dependent fashion. Each data point is the average of 3 technical replicates ($n = 3$). For active compounds **87**, **91**, and control **93**, this experiment was repeated 3 times ($n = 3$) with independent cell cultures. Reported IC_{50}±s.d. values are averages of three independent experiments with standard deviations of the mean.